Quantum-Well-Intermixed Monolithically Integrated Widely Tunable All-Optical Wavelength Converter Operating at 10 Gb/s

Vikrant Lal, *Student Member, IEEE*, Milan L. Mašanović, *Member, IEEE*, Erik J. Skogen, *Member, IEEE*, James W. Raring, *Student Member, IEEE*, Joseph A. Summers, *Student Member, IEEE*, Larry A. Coldren, *Fellow, IEEE*, and Daniel J. Blumenthal, *Fellow, IEEE*

***Abstract*—This letter reports on an InP Mach–Zehnder interferometer semiconductor optical amplifier all-optical wavelength converter monolithically integrated with a sampled grating distributed Bragg reflector laser. The device is fabricated using centered quantum wells to achieve a high modal overlap with the active region. The active and passive waveguide regions are defined using an impurity-free quantum-well intermixing technique. The device is shown to perform error-free at 10-Gb/s data rates with a 30-nm output tuning range. The device's output power is also measured to be >3 dBm across the range.**

***Index Terms*—Mach–Zehnder interferometer (MZI), photonic integrated circuit, quantum-well intermixing (QWI), wavelength conversion.**

I. Introduction

TUNABLE wavelength conversion is a key function for reconfigurable wavelength-division-multiplexing networks. Integration of a tunable laser and an all-optical wavelength converter (WC) on a single chip is necessary to meet performance, yield, cost, and footprint requirements of these networks. As the chip level integration density increases and more components are added on chip increasing the level of functionality, it becomes essential to optimize various active and passive elements for required performance as well as reduce overall chip power consumption. Integrating a laser on the same chip poses additional requirements in terms of on-chip back reflection minimization. Therefore, a robust yet flexible integration platform is required.

Previously, we have reported on the successful demonstration of a monolithically integrated widely tunable all-optical WC (TAO-WC) [1], [2] fabricated using a simple offset quantum-well integration platform. While our devices in this platform exhibited error-free operation at 10 Gb/s over a large tuning range and with 0-dBm converted output power, tradeoffs in the semiconductor optical amplifier (SOA) design stemming from the low optical confinement in the active regions limited the device conversion efficiency and maximum operating speed, when compared to the bulk and centered quantum-well Mach–Zehnder interferometer (MZI)-SOA-WCs [3]. In this letter, we report on the implementation of a centered quantum-well active-region-based tunable WC fabricated using quantum-well intermixing (QWI). QWI provides an attractive solution for postgrowth bandgap control in complex photonic integrated circuits [4], [5]. An impurity-free QWI process [5] is used to spatially define the material bandgap to selectively form active and passive regions. It allows simple fabrication of active–passive centered quantum-well devices without having to resort to complicated growth schemes (selective area growth or butt-joint growth). Furthermore, the value of the confinement factor can be tailored by the choice of the number of quantum wells, and in this implementation is 50% higher compared to [1] and [2]. This platform yields highly saturated and nonlinear SOAs in the WC part, higher output power sampled grating distributed Bragg reflector (SGDBR) laser (relative to [2]), and low-loss low-reflection transitions between active and passive regions of the chip.

The devices presented in this letter exhibit error-free operation at 10-Gb/s data rates with improved conversion efficiency relative to [2], over 30-nm output tuning range, and average converted output powers >3 dBm compared to 0 dBm reported in [2].

II. Device Design and Operation

The tunable WC design consists of a widely tunable SGDBR laser monolithically integrated with an SOA-based MZI WC and is shown in Fig. 1. The operation of these WCs has been described in detail in [1] and [2]. For the devices reported in this letter, an impurity-free vacancy-enhanced QWI process is used to create the active and passive bandgap regions on the chip. The material is selectively ion-implanted with phosphorus ions, and due to the lattice damage caused by the implant, vacancies are created in the material. The vacancies are then diffused through the quantum wells by rapid thermal annealing the sample. The vacancy diffusion causes the quantum well and barrier materials to intermix, resulting in an increase in the bandgap [5]. The implanted material is then etched away to leave the sample

Manuscript received February 2, 2005; revised April 20, 2005. This work was supported by the Defense Advanced Reseach Projects Agency (DARPA)/MTO CS-WDM Program under Grant N66001-02-C-8026.

V. Lal, M. L. Mašanović, E. J. Skogen, J. A. Summers, L. A. Coldren, and D. J. Blumenthal are with the Department of Electrical and Computer Engineering, University of California Santa Barbara, Santa Barbara, CA 93106 USA (e-mail: lal@ece.ucsb.edu; mashan@ece.ucsb.edu; skogen@engineering.ucsb.edu; jsummers@ece.ucsb.edu; coldren@ece.ucsb.edu; danb@ece.ucsb.edu).

J. W. Raring is with the Materials Department, University of California Santa Barbara, Santa Barbara, CA 93106 USA (e-mail: jraring@engineering.ucsb.edu).

Digital Object Identifier 10.1109/LPT.2005.851891

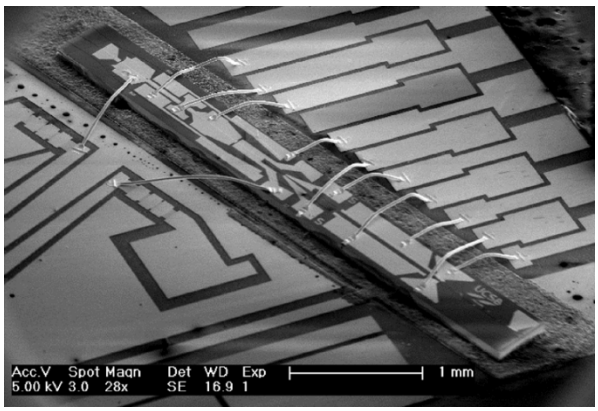

Fig. 1. Scanning electron microscope of the quantum-well-intermixed WC.

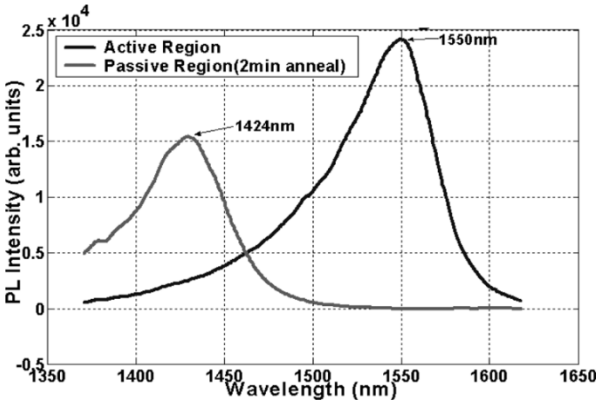

Fig. 2. PL spectra of the active and passive regions on chip after intermixing.

impurity free. This process is described in greater detail in [4] and [5]. Fig. 2 shows the photoluminescence (PL) spectra of the active and passive regions after intermixing. The intermixing process does not lead to any excess loss in the passive waveguides compared to our standard offset quantum-well platform; we measured passive loss around 1.5 dB/mm (or 3.5 cm^{-1}) in both platforms.

The increased confinement factor obtained using centered quantum wells allows us to achieve greater input signal gain, SGDBR power density, and higher phase swing in the MZI [6]. Measurements show continuous-wave power levels (set by the SGDBR laser) of up to 13 dBm in the MZI, compared to 10 dBm in offset quantum-well devices. We also measure a 100% improvement in phase swing as compared to offset quantum-well-based devices for the same input signal and SGDBR power levels, due to the higher modal confinement factor [6]. These improvements can help greatly improve the input dynamic range of these devices and we are working to measure and characterize such benefits.

III. Device Performance

Fig. 3 shows the converted eyes obtained in both modes of operation at pseudorandom binary sequence (PRBS) 2^7-1. We can see clear open eyes with high extinction ratio in both modes of operation. The increased noise at the one-level in the case of the inverting eyes is due to the pattern dependence in the MZI

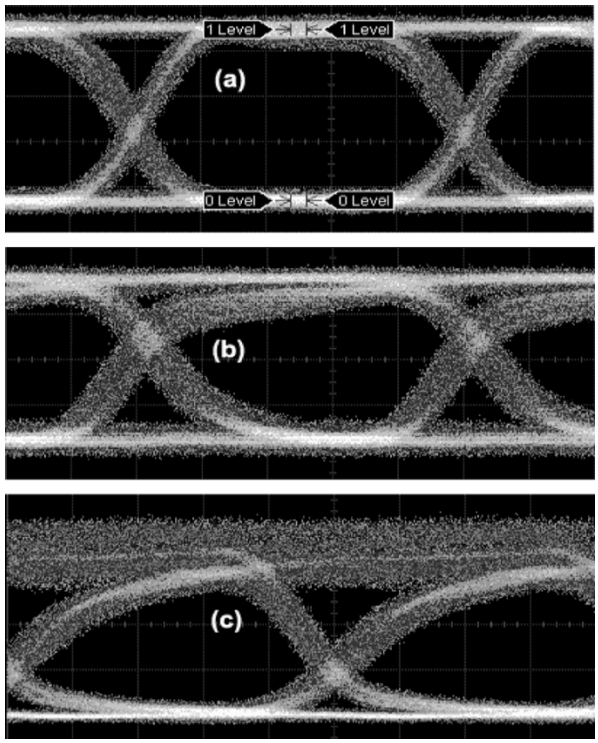

Fig. 3. Eyes of the (a) back-to-back signal and converted signal in (b) noninverting mode (c) inverting mode at PRBS 2^7-1, at 10-Gb/s data rates (time scale on plots 20 ps/div).

SOAs due to a slow gain recovery time. It is not noticeable in the noninverting case since the slow gain recovery is quenched into the zero-level of the converted signal.

We measured the performance of the device for different input and output wavelengths across the C-band at 10-Gb/s data rates. We were able to operate the device from 1530 to 1560 nm, in both the inverting and noninverting modes of operation. Fig. 4(a) shows the error-free operation for both these modes at one set of wavelengths. The erbium-doped fiber amplifiers and thin film filters in our device testing setup limited us to wavelengths below 1560 nm.

Along with the benefit it offers, the increase in the confinement factor also creates additional challenges. The reduction in SOA saturation power results in the enhancement of pattern dependence in the preamplifier and MZI SOAs. This causes a pattern-dependent power penalty for the current generation of devices. As can be seen in Fig. 4(b), for the inverting mode of operation, the power penalty was measured around 1.5 dB for PRBS 2^7-1 and increased to around 4 dB for PRBS $2^{31}-1$, and the bit-error-rate (BER) slope decreased. This was also the case for the noninverting mode of operation.

To estimate the wavelength range of these devices, we performed two different sets of measurements. For the first set, the input wavelength into the device was held constant at 1545 nm, and the device output was tuned from 1530 to 1560 nm. For the second set of measurements, the device output wavelength was help constant at 1545 nm, and the input wavelength to the device was varied from 1530 to 1560 nm. For both sets of measurements, the input data was chosen to be PRBS 2^7-1, and the devices operated in the inverting mode. The measured BER

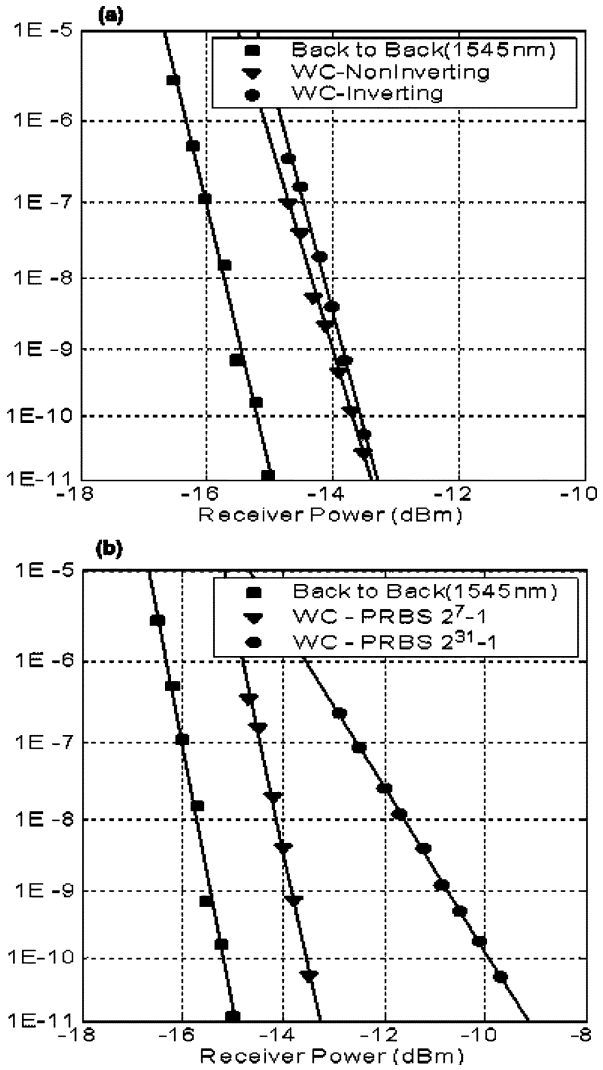

Fig. 4. BER plots for 10-Gb/s operation for (a) noninverting and inverting modes (b) increased power penalty with PRBS $2^{31} - 1$ input. The input wavelength was 1545 nm and output wavelength 1540 nm.

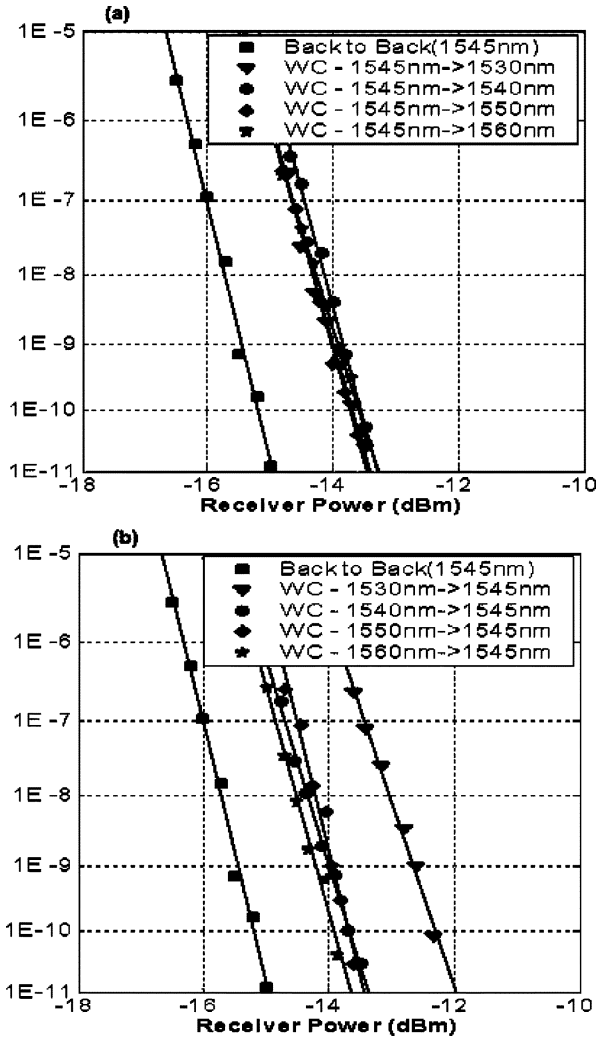

Fig. 5. BER plots for 10-Gb/s operation for (a) input: 1545 nm, output: 1530–1560 nm; (b) input: 1530–1560 nm, output: 1545 nm. The input data was PRBS $2^7 - 1$.

curves are shown in Fig. 5. Device performance degradation is noticeable as the input wavelength approached 1530 nm, which is close gain bandwidth limit for the quantum wells. We expect that these numbers could improve with future device and base epi designs.

IV. Conclusion

We have demonstrated a TAO monolithic WC in InP using a QWI fabrication process. The device exhibits error-free operation at 10 Gb/s. The centered quantum-well-integration platform used to fabricate these devices allows a higher modal overlap with the active region. The increase in the active region confinement factor results in greater phase swing due to cross-phase modulation for the SOAs and also a faster gain recovery lifetime. The operating wavelength range of the device is 30 nm (1530–1560 nm) for both the input as well as output wavelength, and the output power is >3 dBm across the output tuning range.

References

[1] M. L. Mašanović, V. Lal, J. A. Summers, J. S. Barton, E. J. Skogen, L. A. Coldren, and D. J. Blumenthal, "Design and performance of a monolithically integrated widely tunable all-optical wavelength converter with independent phase control," *IEEE Photon. Technol. Lett.*, vol. 16, no. 10, pp. 2299–2301, Oct. 2004.

[2] M. Mašanović, V. Lal, J. A. Summers, J. Barton, E. Skogen, L. Rau, L. Coldren, and D. Blumenthal, "Widely-tunable monolithically-integrated all-optical wavelength converters in InP," *J. Lightw. Technol.*, vol. 23, no. 3, pp. 1350–1362, Mar. 2005.

[3] W. Idler, K. Daub, G. Laube, M. Schilling, P. Wiedemann, K. Dutting, M. Klenk, E. Lach, and K. Wunstel, "10 Gb/s wavelength conversion with integrated multiquantum-well based 3-port Mach–Zehnder interferometer," *IEEE Photon. Technol. Lett.*, vol. 8, no. 9, pp. 1163–1165, Sep. 1996.

[4] E. J. Skogen, J. S. Barton, S. P. Denbaars, and L. A. Coldren, "Tunable sampled-grating DBR lasers using quantum-well intermixing," *IEEE Photon. Technol. Lett.*, vol. 14, no. 9, pp. 1243–1245, Sep. 2002.

[5] ——, "A quantum-well-intermixing process for wavelength-agile photonic integrated circuits," *IEEE J. Sel. Topics Quantum Electron.*, vol. 8, no. 4, pp. 863–869, Jul./Aug. 2002.

[6] M. L. Mašanović, V. Lal, E. J. Skogen, J. S. Barton, J. A. Summers, L. A. Coldren, and D. J. Blumenthal, "Detailed comparison of cross-phase modulation efficiency in offset quantum well and centered quantum well intermixed monolithically integrated widely-tunable MZI-SOA wavelength converters," presented at the Optical Fiber Communication Conf. (OFC 2005), Anaheim, CA, Mar. 2005.